Stable Pentaammineruthenium(III) Complexes of Reductic Acids: Synthesis, Linkage Isomers, and Autoxidation Kinetics

D. M. Bryan, S. D. Pell, R. Kumar, M. J. Clarke,* V. Rodriguez, M. Sherban, and J. Charkoudian

Contribution from the Department of Chemistry, Boston College, Chestnut Hill, Massachusetts 02167. *Received June 1, 1987*

Abstract: Kinetically stable, monodentate, pentaammineruthenium(III) complexes of the reductate ligands ascorbate and tetramethylreductate have been synthesized and characterized spectroscopically and electrochemically, and the autoxidation kinetics have been studied. For all the complexes, axial or rhombic ESR spectra and magnetic susceptibilities in the range 1.8–1.9 μ_B indicate the Ru(III) oxidation state. Both TMRA and ascorbate yield two distinct complexes with closely parallel properties, which form in varying amounts and interconvert depending on the pH of the reaction with an apparent pK_a around 4.2. ^{1}H NMR of the paramagnetic TMRA complexes suggest that the metal ion is closer to one pair of methyl groups in the lower pH form than that in the higher pH form, consistent with the coordination sites of O(2) and O(3) for the low- and high-pH forms, respectively. At low pH this isomerization takes place with a specific rate of 8.0×10^{-4} s^{-1}, and the resulting complex dissociates with a specific rate of 1.0×10^{-4} s^{-1}. At neutral pH the O(2) to O(3) isomerization occurs rapidly, and reductate ligand dissociation proceeds with a half-life of about 6 h. Cyclic voltammetric studies reveal reversible (on the CV time scale) couples ($E°$ values of 0.237 V for $[(Asc)(NH_3)_5Ru]^+$ and 0.306 V for $[(TMRA)(NH_3)_5Ru]^+$), which exhibit a pH dependency consistent with 1e, 1H$^+$ redox processes, suggesting that induced electron transfer to the metal ion occurs upon single-electron oxidation of the ascorbate ligand. Both the reductate complexes and a related squarate complex exhibit an irreversible reduction, apparently due to ligand loss from the Ru(II) complex. The rate of autoxidation of the reductate complexes at pH 7.0 and 25 °C is first order in the ruthenium complex and first order in oxygen concentration. Specific rate constants at 25 °C, ΔH^*, and ΔS^* for the ascorbate and TMRA complexes, respectively, are the following: 5.42 s^{-1} M^{-1}, 60.9 kJ/mol, and −26.6 J/mol K; 2.51 s^{-1} M^{-1}, 69.6 kJ/mol, and −5.5 J/mol K.

Ascorbic acid is a relatively complex reductant (see Figure 1), whose chemical and biological effects often involve the presence of redox-active transition-metal ions.[1] In at least one important enzyme, ascorbate oxidase, the coenzyme appears to interact directly with metal ions at the active site.[2,3] Metal ions capable of undergoing redox reactions are thought to catalyze the autoxidation of ascorbic acid through the formation of intermediate metal–ascorbate–dioxygen complexes.[4] In the Udenfriend system, ascorbic acid catalyzes oxygen activation and oxygen atom insertion through the formation of an initial ascorbate–Fe(III)–dioxygen complex in which electron transfer to dioxygen results.[5] Metal ion catalysis of the autoxidation of ascorbate by Fe(III) and Ru(III) complexes in the presence of DNA has been shown to result in substantial DNA strand cleavage.[6] Recently, an unusual platinum(II)–ascorbate complex was shown to have excellent antitumor properties.[7,8]

While a number of metal ion complexes with ascorbate have been extensively studied[9] and several solid-state structures are available,[10-14] oxygen-bound complexes have not proven to be kinetically stable and so have not been well characterized as to their mode of coordination in solution. Similarly, the autoxidation kinetics of these species have often been described[15-23] but have always been open to speculation as to the specific complex undergoing electron transfer. In an effort to delve into the actual electron transfer to oxygen, in a manner that essentially precludes binding of dioxygen and subsequent inner-sphere electron transfer, we have synthesized a series of stable, monodentate complexes of ascorbic acid and tetramethylreductic acid, a related reductate ligand, and studied their reduction of dioxygen in aqueous solution. Electrochemical studies of these complexes indicate that internal electron transfer to the Ru(III) occurs upon one-electron oxidation of the complex. Tetramethylreductic acid[24] effectively mimics ascorbic acid in many of its redox properties (see Figure 2),[25] while being somewhat more tractable, especially in providing a stronger ^{1}H NMR signal in paramagnetic complexes, such as those reported here. Taking advantage of this, ^{1}H NMR studies of the ruthenium(III) tetramethylreductate complexes illustrate that a pH-dependent linkage isomerization can occur with ascorbate and similar ligands.

(1) Seib, P. A.; Tolbert, B. M. *Ascorbic Acid: Chemistry, Metabolism, and Uses*; American Chemical Society: Washington, DC. 1982.
(2) Kawahara, K.; Suzuki, S.; Sakurai, T.; Nadahura, A. *Arch. Biochem. Biophys.* **1985**, *241*, 179–186.
(3) Kroneck, P. M. H.; Armstrong, F. A.; Merkle, H.; Marchesini, A. In *Ascorbic Acid: Chemistry Metabolism, and Uses*; American Chemical Society: Washington, DC, 1982; pp 223–248.
(4) Martell, A. E.; Khan, M. M. T. In *Inorganic Biochemistry*; Eichhorn, G., Ed.; Elsevier: New York, 1973; pp 654–688.
(5) Martell, A. E. In *Ascorbic Acid: Chemistry, Metabolism, and Uses*; Seib, P. A., Tolbert, B. M. Ed.; American Chemical Society: Washington, DC, 1982; p 153.
(6) Clarke, M. J.; Jansen, B.; Marx, K. A.; Kruger, R. *Inorg. Chim. Acta* **1986**, *124*, 13–28.
(7) Hollis, L. S.; Amundsen, A. R.; Stern, E. W. *J. Am. Chem. Soc.* **1985**, *107*, 274.
(8) Hollis, L. S.; Stern, E. W.; Amundsen, A. R.; Miller, A. V.; Doran, S. L. *J. Am. Chem. Soc.* **1987**, *109*, 3596–3602.
(9) Smith, R. M.; Martell, A. A. *Critical Stability Constants*; Plenum: New York, 1977.
(10) Hearn, R. A.; Bugg, C. E. *Acta Crystallogr., Sect. B: Struct. Crystallogr. Cryst. Chem.* **1974**, *30*, 2705.
(11) Hvoslef, J. Kjellevold, K. E. *Acta Crystallogr., Sect. B: Struct. Crystallogr. Cryst. Chem.* **1974**, *30*, 2711.
(12) Abrahams, S. C.; Berstein, J. L.; Bugg, C. E.; Hvoslef, J. *Acta Crystallogr., Sect. B: Struct. Crystallogr. Cryst. Chem.* **1978**, *34*, 2981.
(13) Hughes, D. L. *J. Chem. Soc., Dalton Trans.* **1973**, 2209.
(14) Hvoslef, J. *Acta Crystallogr., Sect. B: Struct. Crystallogr. Cryst. Chem.* **1969**, *2*, 2209.
(15) Taqui Khan, M. M.; Martell, A. E. *J. Am. Chem. Soc.* **1968**, *90*, 6011.
(16) Jameson, R. F.; Blackburn, N. J. *J. Inorg. Nucl. Chem.* **1975**, *37*, 809.
(17) Taqui Khan, M. M.; Hussain, A.; Ramachandraiah, G.; Moiz, M. A. *Inorg. Chem.* **1986**, *25*, 3023–3030.
(18) Tauqi Khan, M. M.; Martell, A. E. *J. Am. Chem. Soc.* **1967**, *89*, 4176.
(19) Taqui Khan, M. M.; Martell, A. E. *J. Am. Chem. Soc.* **1967**, *89*, 4178.
(20) Hamilton, G. A. *Adv. Enzymol. Relat. Subj. Biochem.* **1969**, *32*, 55.
(21) Taqui Khan, M. M.; Martell, A. E. *J. Am. Chem. Soc.* **1968**, *89*, 7106.
(22) Jameson, R. F.; Blackburn, N. *J. Chem. Soc., Dalton Trans.* **1976**, 534.
(23) McLendon, G.; Martell, A. E. *Coord. Chem. Rev.* **1976**, *19*, 1.
(24) (a) Hesse, C.; Wheeling, B. *Liebigs Ann. Chem.* **1964**, *679*, 100–106. (b) Schank, K. *Synthesis* **1972**, 176–190.
(25) Inbar, S.; Ehret, A.; Norland, K. *Abstracts of Papers*, National Meeting of the Society of Photographic Sciences, Minneapolis, MN, 1987.

0002-7863/88/1510-1498$01.50/0

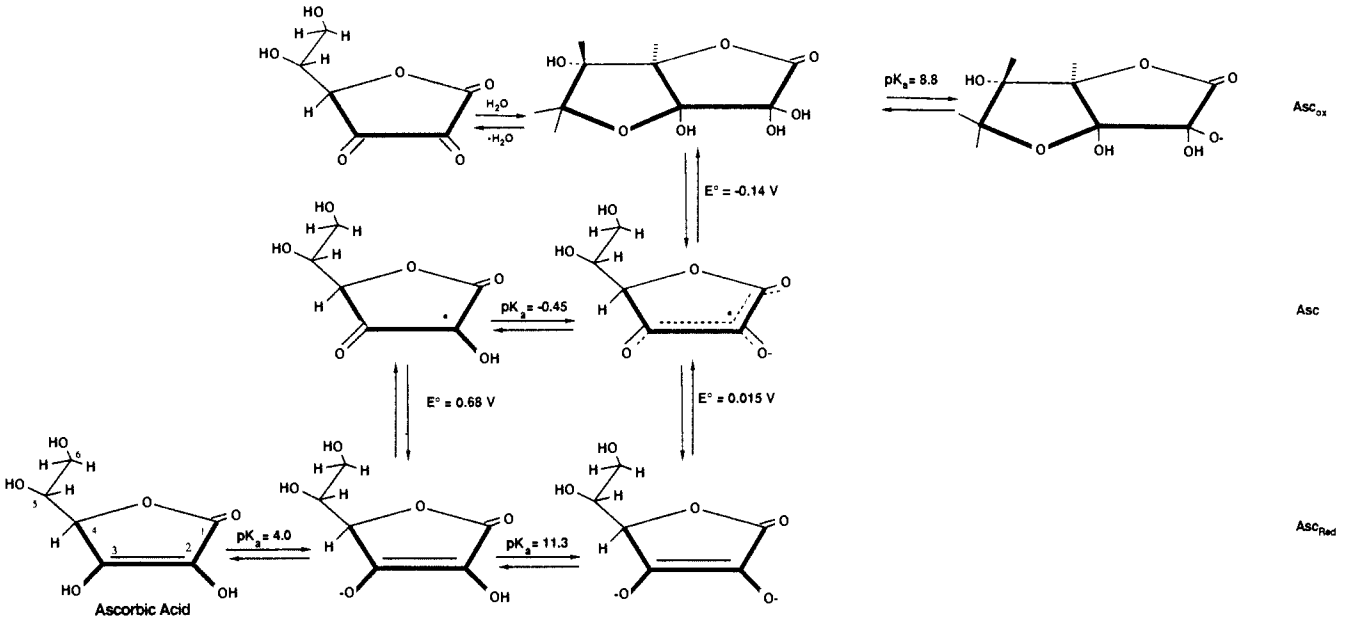

Figure 1. Proton and oxidation-reduction equilibria of ascorbic acid.

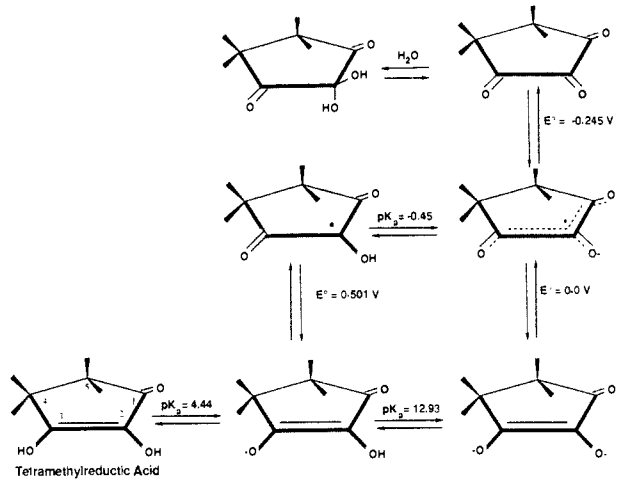

Figure 2. Proton and oxidation-reduction equilibria for tetramethylreductic acid.

Abbreviations: Asc, ascorbic acid; Asc$^{\bullet}$, ascorbate semiquinone; Asc_{ox}, oxidized form of ascorbate; 3-MeAsc, 3-methylascorbate; TMRA, tetramethylreductic acid (2,3-dihydroxy-4,4,5,5-tetramethylcyclopentenone); TMRA$^{\bullet}$, tetramethylreductate semiquinone; $TMRA_{ox}$, oxidized form of tetramethylreductate (4,4,5,5-tetramethylcyclopentane-1,2,3-trione); 3-MeTMRA, 3-*O*-methyltetramethylreductate; Sqr, squarate (3,4-dihydroxy-3-cyclobutene-1,2-dione dianion); TFMS, trifluoromethanesulfonate.

Experimental Section

Synthesis. $[(NH_3)_5RuCl]Cl_2$ was prepared by reduction of $RuCl_3 \cdot 3H_2O$ (Aesar Chemicals) with hydrazine hydrate.[26,27] $[(NH_3)_6Ru]Cl_3$ (Aesar) was dissolved in redistilled water, precipitated by addition of acetone, recrystallized from warm 1 M HCl, and stored in a vacuum desiccator for a few days before use. Trifluoromethylsulfonic acid (HTFMS) from the 3M Co. was vacuum distilled and diluted to 6 M. NaTFMS was prepared by carefully neutralizing a 6 M solution of HTFMS with 3 M NaOH. The neutralized solution was rotary-evaporated to dryness and the solid product recrystallized with ethanol.

3-*O*-Methylascorbic acid was prepared by dissolving 3 g of ascorbic acid in dry methanol (50 mL) and cooling the solution to 0 °C. Diazomethane[28] solution (1 mol equiv) in ether was similarly cooled and added slowly to the ascorbic acid solution so that the temperature did not rise above 5 °C. The solvent was stripped in a rotary vacuum evaporator at 40–50 °C, and a colorless oil was obtained. The crude oil from the reaction was dissolved in a minimum of acetone and loaded onto a silica gel column. An unknown substance was eluted with 20% acetone/petroleum ether (v/v). The 3-*O*-methylascorbic acid was eluted with 45% acetone in petroleum ether.[29] UV (water): λ_{max} 260 nm (ϵ_{max} 9.0 x 10^3 M^{-1} cm^{-1}). ^1H NMR (DMSO): δ 8.9 [C(2) OH], 4.8 [C(4) H], 4.1 [C(3) OCH_3], 2.1 [C(5) H], 1.3 [C(6) H_2].

3-*O*-Methyltetramethylreductic acid was made in the same manner as the 3-*O*-methylascorbic acid (substituting tetramethylreductic acid for ascorbic acid). This compound was recrystallized from a water/acetone mixture. Anal. Calcd for $C_{10}H_{16}O_3$: C, 65.15; H, 8.69. Found: C, 65.15; H, 8.64. Mp: 89–89.5 °C. UV (water: λ_{max} 272 nm (ϵ_{max} 12.7 x 10^3 M^{-1} cm^{-1}). ^1H NMR (DMSO): δ 8.2 [C(2) OH], 4.1 [C(3) OCH_3], 1.02 [C(4 or 5) $(CH_3)_2$], 0.94 [C(4 or 5) $(CH_3)_2$].

(Squarato)pentammineruthenium(III) chloride monohydrate was prepared by direct combination of a twofold excess of squaric acid (Aldrich) with $[Cl(NH_3)_5Ru]Cl_2$ in aqueous solution adjusted to pH 7–8. Purification was effected by ion-exchange chromatography on SP Sephadex eluted with 0.1 M LiCl. Crystals formed from the eluant on standing overnight. Crystalline samples of this compound redissolved only very slowly. Anal. Calcd for $[(C_4O_4)(NH_3)_5Ru]Cl \cdot H_2O$: H, 4.87; C, 13.66; N, 19.91; Ru, 28.7. Found: H, 4.73; C,13.73; N, 18.86; Ru, 28.4. IR (KBr): $\nu_{C=O}$ 1780 cm^{-1}. μ_{eff} = 1.88 μ_B.

(Ascorbato)pentaammineruthenium(III) trifluoromethanesulfonate was prepared by deaerating two vessels by argon bubbling, one containing 20 mL of 1 M NaOH and the other 25 mL of distilled water. $[(NH_3)_5RuCl]Cl_2$ (100 mg) was added into the deaerated water followed by a three- to fivefold excess of L-ascorbic acid (Fisher Scientific). The solution was adjusted to pH 9.0–9.5 with dearated 1 M NaOH. If necessary, additional ascorbic acid was added to lower the pH. The reaction was allowed to proceed at room temperature for 1 h. The components of the resulting blue solution were separated on an inert-atmosphere SP Sephadex column (2 cm diameter × 6–7 cm),[30] which was eluted with (1) deaereated redistilled water (200 mL) to remove the excess ligand and (2) 0.15 M NaTFMS (200 mL), which eluted the desired complex as a dark blue band. The product band was collected in an argon-purged round-bottom flask and the solvent rotary-evaporated off until just dry. The round-bottom flask was then transferred to a glovebox purged with argon. Acetonitrile (25 mL) was added to the flask and swirled for a few minutes before filtering under vacuum. The amorphous blue product was washed with 25 mL of acetonitrile to remove NaTFMS, followed by two more washes with diethyl ether, before dissolving in 1 drop of water followed by the addition of 1 mL of ethanol. The dark blue product, which frequently contained NaTFMS, precipi-

(26) Allen, A. D.; Bottomley, F.; Harris, R. O.; Reinsalu, V. P.; Senoff, C. V. *Inorg. Synth.* **1970**, *12*, 1–7. Fergusson, J. E.; Love, J. L. *Inorg. Synth.* **1972**, *13*, 208–211.

(27) Shreeve, J. Ed. *Inorg. Synth.*, in press.

(28) Arndt, F. *Organic Syntheses*; Wiley: New York, 1945; Collect. Vol. II, p 165.

(29) Shrihatti, V. R.; Nair, P. M. *Indian J. Chem., Sect. B* **1977**, *15B*(9), 861–863.

(30) Creutz, C. Ph.D. Dissertation, Stanford University, 1970, p 26.

tated quickly and was collected by vacuum filtration. The compound is hygroscopic and air sensitive and was stored in a vacuum desiccator or under a dry, inert atmosphere. Anal. Calcd for $[(C_6H_6O_6)(NH_3)_5Ru](F_3CSO_3)$: H, 4.16; C, 16.51; N, 13.75. Found: H, 3.69; 16.55; N, 13.30. IR (KBr): $\nu_{C=O}$ 1650 cm^{-1}. μ_{eff} = 1.83 μ_B.

(Tetramethylreducto)pentaammineruthenium(III) trifluoromethanesulfonate was prepared similarly to the ascorbato complex except that a three- to fivefold excess of tetramethylreductic acid was used.[31] The desired green complex was purified by inert-atmosphere ion exchange on an SP Sephadex column, followed by rotary evaporation, removal of NaTFMS with acetonitrile, and dissolution in 1 drop of water followed by the addition of 1 mL of ethanol. The extremely air-sensitive and hygroscopic material was filtered and stored in a vacuum desiccator. Anal. Calcd for $[(C_9H_{12}O_3)(NH_3)_5Ru](F_3CSO_3)$: H, 5.41; C, 23.86; N, 13.91. Found: H, 5.95; C, 23.93; N, 14.25. ^1H NMR (D_2O, pD 7): δ 4.7 (br) [C(4 and 5) CH_3]. ^1H NMR (D_2O, pD 2.6): δ 6.4 (br) [C(5) CH_3], 12.6 (br) [C(4) CH_3]. IR (KBr): $\nu_{C=O}$ 1640 cm^{-1}.

(3-*O*-Methylascorbato)pentaammineruthenium(III) and (3-*O*-methyltetramethylreductato)pentaammineruthenium(III) were prepared analogously to the ascorbate and TMRA complexes, except that an acetone/water solvent was used to enhance the solubilities of the ligands and the yields were significantly lower. $[Cl(NH_3)_5Ru]Cl_2$ (50 mg) and 3-*O*-methylascorbate or 3-*O*-methyltetramethylreductate (150 mg) were added to 25 mL of argon-purged acetone/water (3:1, v/v), and the pH was raised to 9.5 with 0.1 N NaOH. After 1–2 h the purple solution was rotary-evaporated to remove the acetone. The complex was purified on an SP Sephadex column with 0.2 M LiCl as the eluent. Electronic spectra are listed in Table II.

Equipment. Electronic spectra were obtained by a Perkin-Elmer 575 UV–visible spectrophotometer, which was fitted with a thermostated cell holder capable of holding the temperature constant within ±0.1 °C and interfaced with an IBM XT microcomputer equipped with a digital plotter. The pK_a values of the complexes were determined by spectrophotometric titration using regression analysis with the equation $pK_a = pH - \log [(A_b - A_{pH})/(A_{pH} - A_a)]$, where A_b is the absorbance of the deprotonated form of the complex, A_a is that of the acidic form, and A_{pH} is the net absorbance at a given pH. A combination glass pH electrode, in conjunction with a digital Markson pH/temperature meter (Model 90), was used for all pH measurements. NMR spectra were recorded on a Varian XL300 in D_2O or DMSO with TSP as an internal reference. Infrared spectra were taken on a Perkin-Elmer Model 599B grating spectrophotometer in tetrahydrofuran or KBr pellets. Magnetic susceptibility studies were performed on a Cahn Model 7500 electrobalance. EPR spectra were taken on a Varian E-9 spectrophotometer at liquid nitrogen temperatures in a 1:1 water/ethylene glycol glass.

The concentration of ruthenium in aqueous samples was determined on an Instrumentation Larboratory Model 300 atomic absorption spectrophotometer with a Ru–Pt hollow cathode lamp optimized at approximately 349.9 nm.[32] The standard employed in this analysis was purified, dry $[(NH_3)_3Ru]Cl_3$, which was dissolved in redistilled water, and the pH was adjusted to ~3 with 1.0 M HCl. Working standards, which were 5% in a Cu/Cd suppressant/enhancer solution, were made from the stock solution.[33] Conductivities were measured on a YSI Model 32 conductance meter.

Electrochemical measurements were made with a Princeton Applied Research Model 174A polarographic analyzer equipped with a Houston Instrument Omigraphic 2000 recorder or on a voltammetric apparatus constructed in this laboratory[33] with millimolar solutions of the complexes in 0.1 M LiCl. When very fresh solutions were required, the chromatographic eluent direct from an SP Sephadex column in 0.15 M LiCl, LiTFMS, or NaCl was used. A platinum disk was used as the working electrode, a platinum wire, as the auxiliary electrode, and Ag/AgCl, as the reference electrode. Reduction potentials for reversible couples were determined as the midpoint between the anodic and cathodic peaks of the cyclic voltammetric wave form or as the peak of the square-wave voltammetric current and were internally referenced against the $[(NH_3)_6Ru]^{3+,2+}$ couple. Reported reduction potentials are corrected to the NHE. Pourbaix plots were fitted by nonlinear regression analysis of the appropriate pH-dependent Nernst equation. Oxygen concentrations were determined amperometrically with a Model 20984 Instrumentation Laboratory oxygen electrode with the PAR 174A. The current reading was directly proportional to the partial pressure of oxygen and the amount of dissolved oxygen in the solution. Oxygen concentrations were calibrated at P_{O2} = 0, 0.21, and 1.0 atm with a Henry's law constant of 780 atm/M and corrected for varying temperatures with the appropriate Bunsen coefficients.[34]

HPLC's were run on either a Varian Model 5000 liquid chromatograph equipped with a Varian Vari-Chrom UV–Vis detector and a Cole-Parmer instrument recorder or an IBM Instruments LC9521 isocratic modular pump equipped with a Gilson Model 111B UV detector set at 254 nm and connected to a strip-chart recorder. A 10-cm, 3-μm C-18 column was used with 0.2 M ammonium propionate as the normal eluent (flow rate 1.0 mL/min), but sodium octanesulfonate (4 mg/150 mL) was added for some analyses. The pH of the eluent depended on the form of the complex that was to be chromatographed: pH 7.12 for the blue form of the Asc complex or the green TMRA species, pH 2.0 for the purple Asc or blue TMRA complexes, and pH 4.1 for chromatographing mixtures of both forms of either complex.

Kinetic Measurements. The autoxidation reactions were monitored by following the absorbance band at 276 nm (ascorbate) or 297 nm (TMRA). The rate constants of the autoxidation of the complex were determined from linear least-squares analyses of plots of $\ln(A_t - A_\infty)$ versus time. The oxygen concentration in aqueous solutions of pH 7.0, 0.1 M phosphate buffer, and 0.1 M LiCl at 25 °C was determined amperometrically with an oxygen electrode. A stream of oxygen, which was presaturated with the buffer solution before entering the cell, was bubbled through the solution in the cell until it was saturated with the gas. After the oxygen concentration was determined to be constant, the complex was introduced to the cell by syringe, and the change in absorbance versus time was recorded. The oxidation reaction was repeated in the presence of the oxygen electrode to verify that the oxygen concentration did not vary while the complex autoxidized. Activation parameters were obtained from both Arrhenius and Eyring plots over the temperature ranges 5–45 °C with ascorbate as the ligand and 15–55 °C with TMRA as the ligand.

The rate of autoxidation of both the ruthenium ascorbate and ruthenium TMRA complexes was monitored in the presence of catalase and superoxide dismutase. The catalase (Sigma, 2750 units/mg) was diluted to 55 units/mL. The superoxide dismutase (Sigma, 3200 units/mg) was diluted to 64 units/mL. Each diluted solution also contained 0.17 g of LiCl, 9.75 mL of a phosphate buffer (27.6 g/L NaH_2PO_4), and 15.25 mL of a second buffer solution (28.4 g/L Na_2HPO_4) in a total volume of 50 mL. The cuvette solution consisted of 1 mL of the enzyme solution and 1.5 mL of a solution of 0.1 M LiCl and 0.1 M phosphate buffer (pH 7).

The oxidation of the ascorbate and TMRA complexes of pentaammineruthenium(III) by hydrogen peroxide was studied at 25 °C in 0.1 M phosphate buffer (pH 7.0), 0.1 M LiCl, either 0.026 or 1.28 mM H_2O_2, with the solution in the cuvette being argon-purged before the addition of the complex. The concentration of H_2O_2 was determined by adding 20 mL of 2 M H_2SO_4 to 50.0 mL of the solution to be assayed before titrating to a pink end point with 0.1 M $KMnO_4$.

The rates of isomerization and dissociation of $[TMRA(NH_3)_5Ru]^+$ were determined by monitoring the δ 6.5 ^1H NMR peak as a function of time at pH 2.2 under an argon atmosphere in a sealed NMR tube. The resulting data set was fit by a standard nonlinear regression to the equation $B = [A_0k_1/(k_1 - k_2)](e^{-k_1t} - e^{-k_2t})$,[35] where B is the NMR peak height and A_0 is related to the initial complex concentration. The dissociation of the TMRA complex at neutral pH was monitored by following the disappearance of the δ 4.7 ^1H NMR peak and treating the resulting log A_t/A_0 versus time curve by a standard linear least-squares method.

The rate of formation of (isonicotinamide)pentaammineruthenium(II) from both the ascorbate and TMRA complexes was determined at pH 7.0, 25 °C, and μ = 0.2 M in argon-purged solutions of the complexes to which isonicotinamide (75 mg/25 mL, 0.025 M) was added. The reaction was kept under a blanket of argon and monitored at 480 nm. Comparison samples of (isonicotinamide)pentaammineruthenium(II) and *cis*-bis(isonicotinamide)tetraammineruthenium chloride were prepared by known methods.[36]

Results

Compound Characterization. The combination of $[Cl(NH_3)_5Ru]Cl_2$ with ascorbate or tetramethylreductate yields two distinct complexes depending on the pH at which the reactions are run. Immediately after purification of the ascorbate complex on SP Sephadex at neutral pH, the HPLC of the eluted blue band showed a single peak with a retention time of 1.8 min (capacity

(31) Tetramethylreductic acid was generously supplied by Dr. M. G. Dowling of the Polaroid Corp.
(32) Perkin-Elmer Methods Manual, Ruthenium Standard Conditions, Sept 1976.
(33) Clarke, M. J. *J. Am. Chem. Soc.* **1978**, *100*, 5068–5075.
(34) Battino, R.; Clever, H. L. *Chem. Rev.* **1966**, *66*, 398.
(35) Moore, J. W.; Pearson, R. G. *Kinetics and Mechanism*; Wiley: New York, 1981; p 290.
(36) Diamond, S.; Taube, H. *J. Am. Chem. Soc.* **1975**, *97*, 5921.

Table I. ESR Data of $[(L)(NH_3)_3Ru^{III}]$ Complexes[a]

ligand	pH	g_x	g_y	g_z
Asc	3.0	2.83	2.42	
TMRA	2.25	2.739	2.378	
Asc	8.5	2.74	2.37	1.55
TMRA	8.8	2.705	2.347	1.58
Sqr	7.4	2.628	2.330	1.666

[a]Spectra were taken at liquid nitrogen temperatures in a 1:1 water/ethylene glycol glass.

Table II. UV-Visible Spectra

complex	probable coordination site	pH	λ, nm	$\epsilon \times 10^{-3}$, M^{-1} cm^{-1}
$[(NH_3)_5Ru(Asc)]^+$	O(2)	7.0	284	9.3
			360 (sh)	1.00
			660	0.35
$[(NH_3)_5Ru(Asc)]^{2+}$	O(3)	2.2	260	6.82
			324 (sh)	1.87
			530	0.289
$[(NH_3)_5Ru(TMRA)]^+$	O(2)	7.0	297	13.0
			390 (sh)	1.00
			690	0.50
$[(NH_3)_5Ru(TMRA)]^{2+}$	O(3)	2.0	278	8.92
			360 (sh)	1.31
			550	0.59
$[(NH_3)_5Ru(3\text{-}MeTMRA)]^{2+}$	O(2)	6.2	350	2.28
			550	0.68
$[(NH_3)_5Ru(3\text{-}MeAsc)]^{2+}$	O(2)	6.5	258	2.56
			320 (sh)	0.662
			530	0.176
$[(NH_3)_5Ru(Sqr)]^{2+}$	O(3)	6.5	261 (sh)	18.1
			266	18.3
			322 (sh)	2.18
			354	2.14
			584	1.38

factor, $k' = 0.80$) with an ammonium propionate buffer at pH 7.12 as the eluant. When the purple ascorbate complex was eluted from SP Sephadex at pH 2 and subjected to HPLC with ammonium propionate at pH 2, a single peak with a retention time of 2.0 min ($k' = 0.82$) was observed. HPLC of the ascorbate complex eluted at pH 7 and then adjusted to pH 4.1 produced two HPLC peaks with the ammonium propionate eluant, but when the ion-pairing reagent, octanesulfonate, was added to the solution, three peaks were observed. Onsager plots of the squarate and TMRA complexes showed them to be 1:1 electrolytes at pH 7, which is consistent with their behavior as monopositive ions at $\mu = 0.1$ on ion-exchange columns at this pH.

ESR spectra of complexes are summarized in Table I. The fully deprotonated complexes all exhibited rhombic EPR spectra (figure shown in supplementary material), while the monoprotonated forms of the reductate species exhibited apparently axial spectra. Magnetic susceptibilities for the complexes were in the range 1.8–1.9 μ_B, consistent with Ru(III) species.

Acid hydrolysis of the reductate and squarate complexes in 4 M HCl in air gave solid $[Cl(NH_3)_5Ru]Cl_2$ in 70% yield. Samples of the TMRA complex completely decomposed to $[Cl(NH_3)_5Ru]Cl_2$ and TMRA on standing overnight in 0.01 M HCl under argon as judged by the ^{13}C NMR spectrum of the supernatant and the electronic spectrum of the precipitate. When the blue ascorbate complex was reduced by zinc amalgam at pH 3.0, $[(H_2O)(NH_3)_5Ru]^{2+}$ dissociated and ascorbate ion was identified by its electronic spectrum.

The electronic spectra of the various complexes are summarized in Table II. Both the TMRA and Asc complexes prepared at pH 7 show visible bands around 680 nm for the high-pH form of the complex. The purple complexes synthesized at pH 4 exhibit bands around 550 nm. Spectra of the reductate complexes were recorded from 335 to 800 nm in the range pH 1–7 at an ionic strength of 0.2 to yield pK_a values of 4.2 ± 0.2 for the TMRA complex and 4.25 ± 0.25 for the ascorbate complex. The spectra of the squarate complex was pH independent between pH 0 and 10, indicating its pK_a to be less than 1.

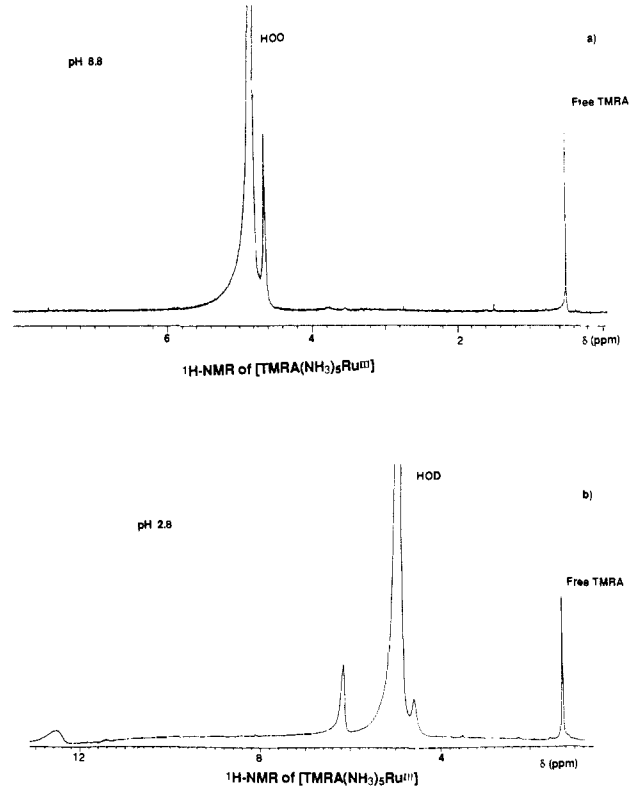

Figure 3. ^1H NMR spectra of both TMRA complexes: (a) high-pH form in D_2O, pD 8.8; (b) Mixture of high- and low-pH forms, pD 2.8. Peak at δ 1.1 is due to free ligand.

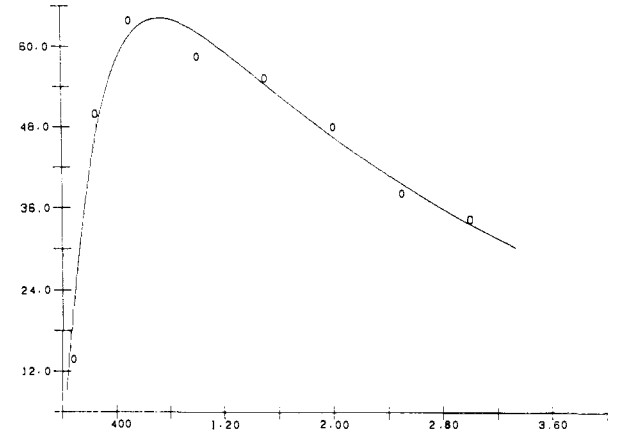

Figure 4. Plot of the ^1H NMR peak height at δ 6.5 versus time after lowering the pH to 2.23.

^1H NMR spectra of the TMRA complex shown in parts a and b of Figure 3 reveal a single peak (δ ~4.7) at neutral pH (which narrows and shifts to δ ~4.0 on cooling to −40 °C in 30% acetone/water at pH ~9); however, two new, broad resonances (δ 6.4, 12.6) grow in at low field with decreasing pH. These are severely broadened and shifted relative to the free ligand, which exhibits a singlet at 1.1 ppm in D_2O. A plot of the peak height of the ^1H NMR resonance at δ 6.4 for the low-pH form of the TMRA complex versus time is shown in Figure 4. A fit of this curve yielded a rate constant of 8.0×10^{-4} s^{-1} for the conversion from the high-pH form to the low-pH form. The subsequent dissociation of the complex at this pH (2.23) occurs with a specific rate of 1.0×10^{-4} s^{-1}. Figure 5 shows the fraction of the complex in the high-pH form as a function of pH. Since these points were taken after sufficient time for the system to approach equilibrium, the relative abundance of the two forms is clearly under pH control with an effective pK_a (4.2) for the process near that of the spectrophotometrically determined pK_a for the high-pH form.

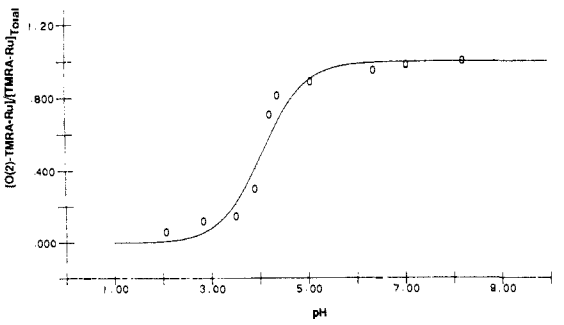

Figure 5. Plot of the fraction of the high-pH form of $[(TMRA)(NH_3)_5Ru]^+$ versus pH as determined from the ratio of the ^1H NMR peaks at 4.4 and 6.4 ppm, showing how the equilibrium is affected by pH. Effective pK_a as determined from this plot is 4.16.

Attempts were made to observe the rate of conversion from the low-pH form to the high-pH form by suddenly neutralizing a sample, which had been at low pH sufficiently long to be nearly completely converted to the low-pH form. However, these samples had almost completely lost the peak at δ 6.4, before the ^1H NMR measurement could be made. Consequently, the half-life for this reaction at neutral pH can only be estimated as being about 1–2 min. The loss of TMRA from the complex in neutral solution proceeded slowly with a rate of 3.3×10^{-5} s^{-1}.

Electrochemistry. Cyclic voltammetric scans for $[(TMRA)(NH_3)_5Ru^{III}]^+$ are shown in Figure 6. The wave exhibited in Figure 6a is attributed to the oxidation of the ligand. A slight broadening in the oxidation wave centered around 400 mV, which grew in on allowing the sample to stand or upon reduction at more negative potentials, suggests some degree of decomposition. A plot of applied voltage versus log $[(i_d - i)/i]$, where i is the cyclic voltammetric current over the initial portion of the anodic scan and i_d is the diffusion-limited current for the couple illustrated in Figure 6a, yielded a slope of 59 ± 12 mV (n = 7, two different samples) consistent with a single-electron transfer. Similarly, peak separations and shapes resembled those of the single-electron, internal reference couple, $[(NH_3)_6Ru]^{2+,3+}$. The Pourbaix diagram for this couple in $[(TMRA)(NH_3)_5Ru]^+$ is shown in Figure 7. The slope in the pH-dependent region is 59 mV/pH, also consistent with a redox process involving the transfer of a single electron coupled with a single proton. The reduction potential for the process in the pH-independent region is 306 ± 6 mV. In the Pourbaix diagram the ascorbate complex is similar and exhibits a pH-independent potential of 237 ± 3 mV.

Both the TMRA and Asc complexes exhibited a similar, irreversible couple centered around −260 mV for the TMRA complex and −300 mV for the ascorbate at neutral pH. This is attributed to reduction of the metal to Ru(II) followed by rapid dissociation of the reductate ligand to yield $[(H_2O)(NH_3)_5Ru^{II}]^{2+}$. As expected a new wave grows in the range expected for the $[(H_2O)(NH_3)_5Ru^{II,III}]$ couple (−30 mV).

A wave centered at −93 ± 4 mV on an HMDE was evident in cyclic voltammetric and square-wave scans of the squarate complex and is attributed to the reduction of the metal ion. The position

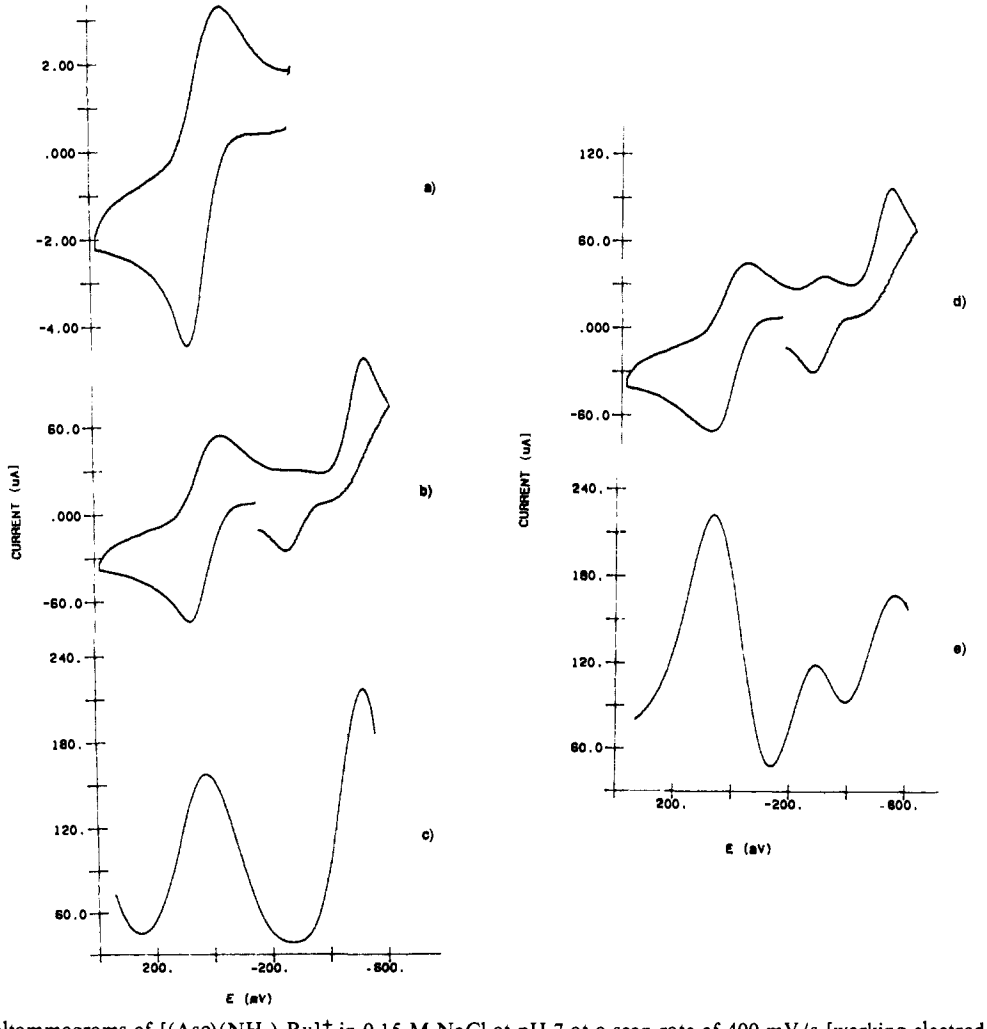

Figure 6. Cyclic voltammograms of $[(Asc)(NH_3)_5Ru]^+$ in 0.15 M NaCl at pH 7 at a scan rate of 400 mV/s [working electrode, Pt disk; reference electrode, Ag/AgCl (scale relative to this electrode)]: (a) scan showing $[(Asc_{ox})(NH_3)_5Ru^{II}]^{2+} + e^- \rightleftarrows [(Asc)(NH_3)_5Ru^{III}]^+$ couple; (b) scan showing additional $[(Asc)(NH_3)_5Ru^{III}]^+ + e^- \rightleftarrows [(Asc)(NH_3)_5Ru^{II}]$ irreversible couple; (c) square-wave voltammetry beginning at 300 mV and scanning cathodically illustrating presence of only the couples indicated in a and b; (d) subsequent scan illustrating the presence of the couple, $[(OH)(NH_3)_5Ru^{III}]^+ + e^- + H^+ \rightleftarrows [(H_2O)(NH_3)_5Ru^{II}]$, which grows in as a result of dissociation of $[(Asc)(NH_3)_5Ru^{II}]$; (e) square-wave voltammetry beginning at −600 mV and scanning anodically showing couples indicated in a, b, and d.

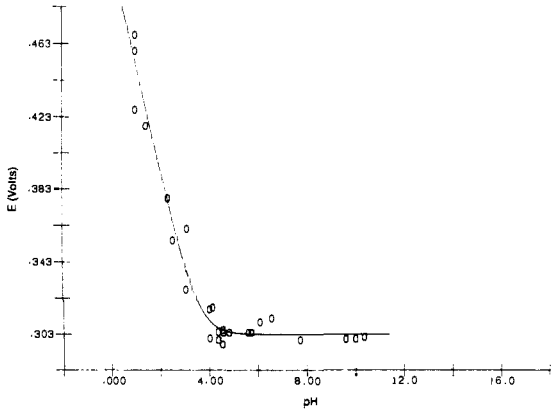

Figure 7. Pourbaix diagram for $[(TMRA_{ox})(NH_3)_5Ru^{II}]^{2+} + e^- + H^+ \rightleftarrows [(TMRA)(NH_3)_5Ru^{III}]^+$.

of this peak was independent of pH between pH 2 and 12 and increased below pH 2, indicating the pK_a of the Ru(II) complex to be ~2. The CV waveform was almost completely irreversible on carbon paste electrodes at low pH, and only somewhat irreversible on platinum, mercury, or carbon paste electrodes at neutral pH and scan rates around 400 mV/s, indicating dissociation of the complex upon reduction. An irreversible reduction postwave, attributed to adsorption of the oxidized complex, was observed to grow in at −175 mV with decreased scan rates. Brief electrolysis of solutions at −100 mV to which isonicotinamide had been added yielded a current peak around 400 mV, which increased with increasing electrolysis time. This is consistent with the formation of $[(Isn)(NH_3)_5Ru]^{2+}$ from the $[(H_2O)(NH_3)_5Ru^{II}]^{2+}$ released by the electrolysis.

Autoxidation Kinetics. In order to determine whether the reductate complexes yield $[(H_2O)(NH_3)_5Ru]^{2+}$ upon decomposition, isonicotinamide (0.025 M) was added to argon-purged solutions of the complex at pH 7. The complex $[(Isn)(NH_3)_5Ru]^{2+}$ is known to form from $[(H_2O)(NH_3)_5Ru]^{2+}$ with a specific rate constant of 0.105 M^{-1} s^{-1}.[37] Under these conditions the ascorbate complex yielded $[(Isn)(NH_3)_5Ru]^{2+}$ with a k_{obsd} of 2.14×10^{-5} s^{-1}, while for the tetramethylreductic acid complex $k_{obsd} = 5.7 \times 10^{-6}$ s^{-1}. Since these specific rates are markedly slower than the pseudo-first-order rate constant for isonicotinamide complexation of $[(H_2O)(NH_3)_5Ru]^{2+}$ (2.6×10^{-3} s^{-1}), decomposition and reductate reduction of the complex to yield $[(H_2O)(NH_3)_5Ru]^{2+}$ is rate-limiting. The half-lives for these processes (9.6 h for the ascorbate and 34 h for the TMRA complex) indicate these complexes to be relatively stable with respect to decomposition and formation of $[(H_2O)(NH_3)_5Ru]^{2+}$ in the absence of air at neutral pH. At pH 7, air oxidation of $[(Asc)(NH_3)_5Ru]^+$ has a half-life of 7.0 min, while that of $[(TMRA)(NH_3)_5Ru]^+$ is 16 min. Consequently, autoxidation, which proceeds fairly rapidly, is not subsequent to complex decomposition.

For $[(Asc)(NH_3)_5Ru]^+$, the observed autoxidation specific rate (k_{obsd}) at $P_{O2} = 0.21$ atm and 25 °C was $(1.7 \pm 0.3) \times 10^{-3}$ s^{-1} between pH 7 and 11 and decreased to 0.9×10^{-3} s^{-1} at pH 4.33. Plots of ln $(A - A_\infty)$ versus time were usually linear over 2–3 half-lives. The inset in Figure 8 shows that the initial rates of autoxidation are linearly dependent on the concentration of the ruthenium complex [data in supplementary material (Tables Is and IIs)]. Plots of k_{obsd} versus oxygen concentration (Figure 8) are also linear (data in Tales IIIs and IVs), indicating the overall rate law to be

$$d[Ru\text{-}L]/dt = k[Ru\text{-}L][O_2]$$

where Ru-L is $[(Asc)(NH_3)_5Ru]^+$ or $[(TMRA)(NH_3)_5Ru]^+$. Specific rate constants at 25 °C for the ascorbate and TMRA complexes, respectively, are 5.42 ± 0.2 and 2.51 ± 0.06 s^{-1} M^{-1}.

Eyring and Arrhenius plots for the autoxidation of the ruthenium ascorbate complex and the ruthenium tetramethylreductate

(37) Shepherd, R. E.; Taube, H. *Inorg. Chem.* **1973**, *12*, 1392–1401.

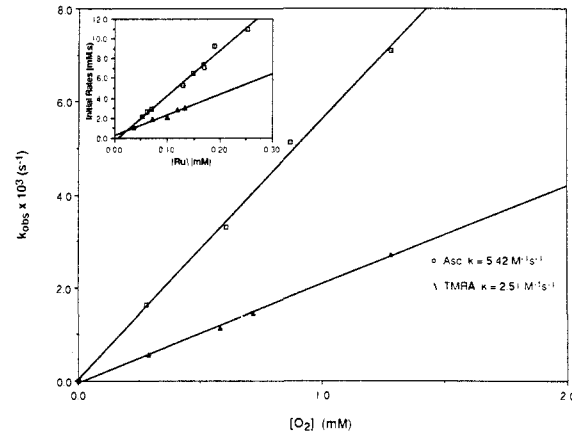

Figure 8. Dependence of the rate constant k_{obsd} for the autoxidation of $[(Asc)Ru(NH_3)_5]^+$ and $[Ru(NH_3)_5(TMRA)]^+$ on dissolved oxygen concentration at 25 °C in 0.1 M LiCl and 0.1 M phosphate buffer (pH 7). Symbol codes: ⊡, $[(Asc)(NH_3)_5Ru]^+$ = 0.183 mM; Δ, $[(TMRA)(NH_3)_5Ru]^+$ = 0.123 mM. Inset: The initial velocities (V_{init}) for the autoxidation of $[Ru(NH_3)_5(Asc)]^+$ and $[Ru(NH_3)_5(TMRA)]^+$ at various concentrations of the complexes (pH 7.0, 0.1 M phosphate buffer, 25 °C, 0.1 M LiCl). Symbol codes: ⊡, $[(Asc)(NH_3)_5Ru]^+$; Δ, $[(TMRA)(NH_3)_5Ru]^+$.

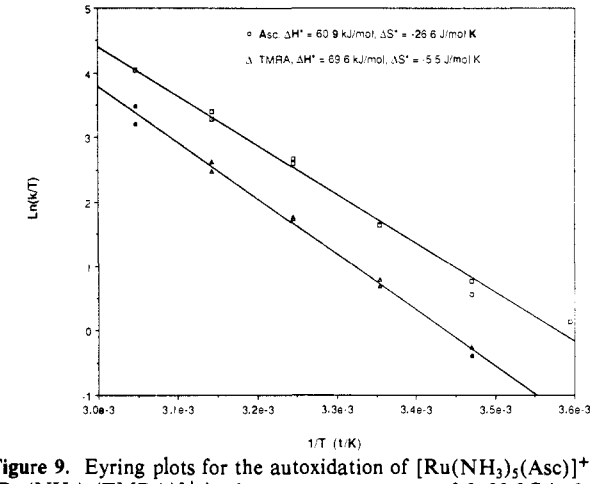

Figure 9. Eyring plots for the autoxidation of $[Ru(NH_3)_5(Asc)]^+$ and $[Ru(NH_3)_5(TMRA)]^+$ in the temperature range of 5–55 °C in 0.1 M LiCl and 0.1 M phosphate buffer (pH 7). Symbol codes: ⊡, $[(Asc)(NH_3)_5Ru]^+$; Δ, $[(TMRA)(NH_3)_5Ru]^+$. Duplicate data were obtained at approximately $P_{O_2} = 0.21$ and $P_{O_2} = 1.0$.

complex are shown in Figure 9 (data in Tables Vs). Activation parameters for the autoxidation of the two complexes are the following: $[(Asc)(NH_3)_5Ru]^+$, $\Delta H^\ddagger = 60.9 \pm 2.3$ kJ/mol, $\Delta S^\ddagger = -26.6 \pm 1.2$ J/mol K; $[(TMRA)(NH_3)_5Ru]^+$, $\Delta H^\ddagger = 69.6 \pm 1.7$ kJ/mol, $\Delta S^\ddagger = -5.54 \pm 0.16$ J/mol K.

In order to determine whether superoxide or peroxide was participating in the oxidation of the reductate complexes, reactions were monitored in the presence of superoxide dismutase and catalase. The rates were unaffected by the presence of either enzyme (see Table VIs). The observed rate constants for oxidation of the complexes by hydrogen peroxide determined at concentrations comparable to those of dissolved oxygen at $PO_2 = 0.21$ (0.26 mM) and 1.0 atm (1.28 mM) (data in Table VIIS) show that the rate of peroxide oxidation is 0.2–0.6 that of the autoxidation rate.

Discussion

Structure. The dianionic ascorbate ion (see Figure 1) is a potentially bidentate ligand capable of reacting with metal ions of coordination number 4 or 6 to form a series of complexes $ML^{(n-2)+}$ and $ML_2^{(n-4)+}$, or $ML^{(n-2)+}$, $ML_2^{(n-4)+}$, and $ML_3^{(n-6)+}$. Stability constants for metal complexes in which the ascorbate is monoprotonated are generally less than 10^2, while those for the dianionic ligand are usually less than 10^4. Monoprotonated as-

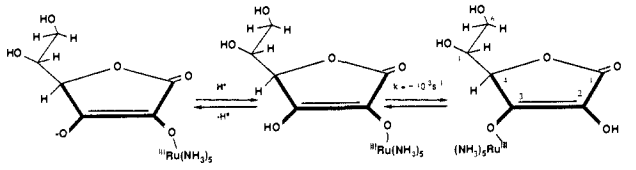

Figure 10. Proposed linkage isomers of $[(Asc)(NH_3)_5Ru]^+$.

corbate complexes are fairly weak because of the low negative charge on the ascorbate anion and resonance delocalization over O(1) and O(3). Coordination generally occurs at O(3) with hydrogen or direct bonding to O(2). The metal complexes of the completely deprotonated ligand are generally assumed to be bidentate chelates with the metal ion bound to O(2) and O(3); however, coordination to O(2) and O(1) is also possible because of the delocalization of the negative charge between the oxygens at the 1- and 3-carbon atoms.[5]

Stable monodentate complexes of the reductate ligands as well as the similar squarate ion are easily prepared by direct combination with $[Cl(NH_3)_5Ru]Cl_2$ at pH levels where the ligands are at least partially ionized. In the case of the reductate ligands, which may reduce the starting material to form $[(H_2O)(NH_3)_5Ru^{II}]^{2+}$, synthesis may be facilitated by redox catalysis. For all types of ligands, when the reactions were run at pH 7, only a single monomeric species was produced as indicated by both ion-exchange and HPLC chromatographies; however, in the case of the reductates, when the reactions were run at pH 4.1, both types of chromatography indicated two products. The acid hydrolysis experiments indicate that the metal is coordinated as $[(NH_3)_5Ru]^{3+}$ in both the high- and low-pH forms of all the complexes. Supplementary to this is the appearance of $[(H_2O)(NH_3)_5Ru^{II}]^{2+}$ upon reduction of these complexes either chemically or electrochemically. Finally, the ESR and magnetic susceptibility data are consistent with a Ru(III) ion in an axial or rhombic environment and a crystal structure of the model complex $[(Sqr)(NH_3)_5Ru]Cl\cdot H_2O$ clearly shows the pentaammineruthenium ion coordinated in monodentate fashion to an anionic oxygen on the ligand.[38] Consequently, since Ru(III) is a substitution-inert, invariably six-coordinate metal ion, both the monoprotonated and dianionic reductate complexes appear to contain a monodentate metal center. However, as is apparent in the crystal structure of the squarate complex, hydrogen bonding involving coordinated ammines probably occurs to an adjacent reductate oxygen.

The nature of the two forms of the complexes, whose relative abundances depend on pH, can be explained by a straightforward interpretation of the ^1H NMR spectra of the TMRA complex (cf. Figures 3 and 10). At neutral pH only a single, broad proton resonance is observed in this paramagnetic ion. Consequently, the four methyl groups must be equivalent under these conditions on the NMR time scale. This can occur only if the metal ion is coordinated to O(2) of TMRA. Since the C(2)–O(2)–Ru bond would be expected to be bent, such bonding does not yield the minimally required C_{2v} symmetry. However, rapid rotation of the ruthenium center around the C(2)–O(2) bond provides the necessary "average" symmetry on the NMR time scale. Bonding at the O(2) site in the fully deprotonated reductate ligands is to be expected, since this site is substantially more basic than O(3).

When the O(2)-bound TMRA complex is placed in a low-pH medium, the ^1H NMR spectrum gradually changes. Two peaks are finally obtained, one of which is substantially broader and highly downfield shifted (see Figure 3). This strongly implies that the paramagnetic center is now located closer to one pair of methyl groups. This can occur if protonation of the ligand takes place at the most basic site, O(2), and displaces the metal ion, which then binds at the available anionic O(3). Such pH-dependent linkage isomerizations involving Ru(III) ammine ions are now well-known for glycine,[39] ethylglycinate,[40] hypoxanthine,[41] and adenine[33] ligands and occur with comparable rates.

The UV–vis spectra of all the complexes exhibited a broad, absorption band centered in the 550–650-nm region as well as a more intense band centered at 350–380 nm. Since these shift toward higher energy on protonation (cf. Table II), they are attributed to ligand π to metal d_π charge-transfer (LMCT) transitions. The similarity in spectra between the monoprotonated O(3)-bound complexes and the 3-methylreductate complexes (cf Table II), which preclude binding at O(3), indicates that protonation and not the metal coordination site is the major factor in determining their spectra. This also accounts for the difficulty in monitoring the linkage isomerization by visible spectroscopy. The presence of low-energy, relatively intense LMCT bands implies overlap of the metal d_π and ligand π-orbitals and some degree of π-bonding.

While pK_a values for the complexes ($\sim$4.2) are similar to those of the free ligands for deprotonation at the same site, this is a result of a cancellation of effects involving an increase in acidity owing to the presence of the metal ion and an increase in basicity arising from the ligand being anionic, rather than neutral.[42] Consequently, a direct comparison of the effect of a Ru(III) at O(2) on increasing the acidity at O(3) cannot be made, since the acidity of a proton residing at O(3) on the monoprotonated ligands has not been measured. Nevertheless, it is probably only somewhat more acidic than the observed pK_{a2} (see Figure 1), i.e. in the range 10–11. The increase in acidity of this site on coordination of $[(NH_3)_5Ru]^{3+}$ at O(2) is then consistent with a Ru(III) being located 3–4 Å away.[41]

Electrochemistry. The slopes of the log $[(i_d - i)/i]$ versus applied voltage and Pourbaix plots (Figure 7) and the similarity in cyclic voltammetric waveforms to that for $[(NH_3)_6Ru]^{2+,3+}$ indicate that the reductate complexes provide a single electron on oxidation. However, it is likely that the reductate ligand actually undergoes a net two-electron oxidation, with the second electron being transferred intramolecularly to the Ru(III). Such induced electron transfer has been observed in a number of systems, including catecholato complexes of Ru(III).[42] The red, metastable species formed on oxidation of these complexes may then have the formulation $[(L_{ox})(NH_3)_5Ru^{II}]^{2+}$, where L_{ox} is dehydroascorbate or dehydrotetramethylreductate. Since both of these form hydrates (see Figures 1 and 2) and coordinated Ru(II) is known to suppress ligand hydration,[43] it is likely that this equilibrium is also affected by the metal ion.

While direct comparisons may be complicated by the hydration equilibria of the oxidized reductates, the two-electron reduction potentials for the fully deprotonated reductate ligands (see Figures 1 and 2) are increased by approximately 300 mV, owing to Ru(III) coordination. This increase can be attributed to the proximity of the metal ion's positive charge and, probably, to a degree of π-bonding between the ligand and metal, delocalizing some electron density away from the reductate.

The 100–200-mV difference in the reduction potentials assigned to the Ru(III,II) couple in the reductate complexes and the squarate complexes is notable, since the ligands are similar in charge and mode of coordination. This probably arises from the reducing properties of the reductate ligands effecting a partial electron transfer to the Ru(III) via π-d_π binding. Such transfer onto the metal ion occurs frequently with Ru(III) and makes electron transfer thermodynamically more difficult.[33] Following reduction, both types of complexes dissociate fairly rapidly to yield $[(H_2O)(NH_3)_5Ru^{II}]^{2+}$.

Oxidation Kinetics. Kahn and Martell proposed that, *in an inert atmosphere*, Fe(III) and Cu(II) directly oxidize ascorbate to dehydroascorbic acid and suggested a mechanism in which the metal ion first binds to the monoprotonated ascorbate. An electron is then transferred from the ascorbic acid to the metal ion, yielding

(38) Pell, S. D.; Clarke, M. J.; Davis, M. A., unpublished work.
(39) Diamond, S.; Taube, H. *J. Am. Chem. Soc.* **1975**, *97*, 5921.
(40) Yeh, A.; Taube, H. *J. Am. Chem. Soc.* **1980**, *102*, 4725–4729.
(41) Kastner, M. E.; Coffey, K. F.; Clarke, M. J.; Edmonds, S. E.; Eriks, K. *J. Am. Chem. Soc.* **1981**, *103*, 5747–5752.
(42) Pell, S. J.; Salmonsen, R.; Abelliera, A.; Clarke, M. J. *Inorg. Chem.* **1984**, *23*, 385–387, and references therein.
(43) Zanella, A.; Taube, H. *J. Am. Chem. Soc.* **1971**, *93*, 7166–7173.

$M^{(n-1)+}$ and the radical anion of ascorbate upon dissociation. Another M^{n+} subsequently binds to the ascorbate radical anion, and a second electron is transferred intramolecularly to the metal ion, with the resulting complex dissociating to dehydroascorbic acid and a reduced metal ion.[18] Consistent with this, these reactions are first order in ascorbate monoanion and first order in metal chelate. It was further suggested that the mechanism of oxidation of ascorbic acid by varioius chelates of Fe(III) and Cu(II) is similar to that of the aquometal ion; however, the rates are very much slower. The rates decrease rapidly as the stabilities of the metal chelates increase but do not correlate with the rates that would be predicted through a mechanism involving the equilibrium dissociation of metal chelate to the free (aquo) metal ion. This implies either ascorbate addition to expand the coordination sphere or (more likely) dissociation of an arm of the polydentate ligand followed by ascorbate binding prior to electron transfer.

Complex ions, such as aquo ions, with coordination sites that may bind oxygen appear to catalyze the autoxidation of ascorbate differently from those in which oxygen coordination may be prevented by chelating ligands. Autoxidations involving the former type of complex with either Cu^{II}_{aq} or Fe^{III}_{aq} exhibit overall third-order behavior, first order in ascorbate, the metal ion, and (above 15 mM) dioxygen.[19] This type of rate law suggests the formation of an intermediate ascorbate–metal ion–dioxygen complex in which the rate-determining electron transfer takes place. Although the bonding between the metal ion and the dioxygen in the intermediate dioxygen complex would seem to be extremely weak, Hamilton has suggested it may be resonance stabilized.[20] Accordingly, the rate-determining electron-transfer step is indicated as occurring through an ionic shift of two electrons to give directly a Cu(II) complex containing weakly coordinated dehydroascorbic acid and a more strongly coordinated hydroperoxide donor. This complex rapidly dissociates to the free metal ion, H_2O_2, and the oxidation product. It is also reasonable to illustrate the redox reaction as occurring in two successive one-electron transfers with the formation of an intermediate complex in which Cu(II) is bound to a deprotonated ascorbate radical anion and a superoxide anion.

Kahn and Martell also found that the rates of ascorbate oxidation by metal chelates, such as iminobis(acetato)copper(II), EDTA–Cu(II), NTA–Fe(III), and EDTA–Fe(III), were independent of molecular oxygen concentration and much slower than those observed with free (aquo) metal ions and that reaction rates decreased with increased stability of the copper or iron chelates involved.[21] In these reactions it was suggested that the deprotonated ascorbate radical anion and the ligand are simultaneously bound to the reduced metal ion and remain combined with the metal ion when it is reoxidized to the higher valence state. After the second electron transfer, the resulting dehydroascorbic acid is such a weak ligand that it readily dissociates, and the simple metal chelate in which the metal ion is in its lower valence state is reoxidized by molecular oxygen to regenerate the catalyst.

Jameson and Blackburn accounted for a half-order dependence in the rate of Cu(II)–catalyzed autoxidation of ascorbic acid on molecular oxygen by suggesting an alternative mechanism in which the formation of a binuclear Cu(II) complex of the ascorbate anion occurs followed by the formation of an intermediate peroxo type Cu(II)–dioxygen–ascorbate complex.[22] Their data suggest a variety of rate behavior depending on the nature of the supporting electrolyte. Analogous complexes have also been observed for cobalt dioxygen systems.[23]

The first-order dependence in both the complex and dissolved oxygen for the rate laws reported here is consistent with those for Cu^{II}_{aq} and Fe^{II}_{aq}, in which the formation of the reductate complex was rate-limiting. When stable reductate complexes are preformed, this step is eliminated and the oxidation step determines the rate. However, in contrast to the case with aquo ions, there remains no open coordination site for the oxygen, so that electron transfer most likely proceeds in an outer-sphere fashion. Autoxidation catalyzed by metal chelates also appears to be limited by the formation of a binary, metal–ascorbate species. Consequently, the rates reported here represent the first direct measures of the actual electron transfer to oxygen. Since a single-electron, electrochemical couple was observed for these complexes around 200–300 mV, it is likely that the initial autoxidation step also proceeds by a single-electron transfer to initially yield superoxide and a dehydroreductate–ruthenium(II) species. However, the ultimate oxygen reductant product is mostly likely H_2O_2 arising either from superoxide disproportionation or superoxide attack on the oxidized, red complex. When the Marcus relation is employed a value of $\sim 1.6\ M^{-1}\ s^{-1}$ was obtained for the outer-sphere autoxidation rate of the ascorbate complex by using the following assumptions: (1) a self-exchange rate for the ascorbate complex of $\sim 10^4\ M^{-1}\ s^{-1}$, which is higher than that for $[(NH_3)_6Ru]^{2+,3+}$ but lower than those for complexes with aromatic ligands, and (2) an intermediate value of $\sim 10^3\ M^{-1}\ s^{-1}$ for the self-exchange rate of O_2/O_2^- and an $E°$ for this couple of −0.155 V.[44] Given the possible variations in the assumed values, this estimation agrees very well with the observed rate of $2.51\ M^{-1}\ s^{-1}$.

Table III. Activation Parameters for the Oxidation of Ascorbate by Molecular Oxygen Catalyzed by Selected Metal Ions

metal chelate	$\Delta H^‡$, kJ/mol	$\Delta S^‡$, J/(mol·K)	$\Delta G^‡$, kJ/mol	ref
$Ru^{III}(NH_3)_5$	60.9	−26.6	68.8	this work
Co^{II}–salen	58.16	−40.6	70.2	*a*
Cu^{II}_{aq}	64.8	58.6	47.3	*b*
Fe^{III}_{aq}	54.39	8.40	51.9	*a*
VO_2^+	57.7	17.1	52.7	*c*

[a] Tsukahara, K.; Ushio, H.; Yamamoto, Y. *Chem. Lett.* **1980**, 1137–1140. [b] Taqui Khan, M. M.; Martell, A. E. *J. Am. Chem. Soc.* **1967**, *89*, 4176. [c] Taqui Khan, M. M.; Martell, A. E. *J. Am. Chem. Soc.* **1968**, *90*, 6011.

Since the autoxidation of ascorbate and TMRA complexes was not inhibited by the addition of either catalase or superoxide dismutase,[45] it appears that neither superoxide nor peroxide is important as intermediates in the autoxidation of these complexes. While hydrogen peroxide does oxidize reductate complexes, these rates are significantly lower than that for autoxidation at the same concentrations, and since the concentration of hydrogen peroxide produced in autoxidation is always less than that of molecular oxygen, its contribution to the overall rate is not measurable. Hence, autoxidation of these complexes proceeds by direct, outer-sphere electron transfer to molecular oxygen.

The slightly high activation enthalpy relative to ascorbate autoxidation catalyzed by other metal ions (see Table III) is probably related to a decreased driving force for the reaction, owing to π-bonding to the metal and concomitant resonance stabilization of the reduced ascorbate. The negative activation entropy, as opposed to the entries for Cu(II), Fe(III), and VO_2^+, probably derives from the latter ions forming an inner-sphere complex with oxygen in the transition state, whereas outer-sphere electron transfer occurs in the present case.

Amminеruthenium(III) complexes with halide or anionic oxygen ligands often exhibit good antitumor activity.[46] Unlike the squarate complex, which was effective against several tumor types, the ascorbato complex was not.[47] A possible mechanism for the antitumor activity of these and similar ruthenium complexes is that they are activated by reduction in vivo, yielding $[(H_2O)(NH_3)_5Ru^{II}]^{2+}$ following ligand dissociation. Indeed, active complexes of this type have reductions potentials that are biologically accessible. The difference in Ru(III,II) reduction potentials between the ascorbate and squarate complexes makes it much more likely that the latter will be reduced in vivo than the former. Conseqeuntly, the squarate complex will produce a much greater quantity of $[(H_2O)(NH_3)_5Ru^{II}]^{2+}$, which actively binds to biological substrates, such as nucleic acids.[6]

(44) Stanbury, D. M.; Haas, O.; Taube, H. *Inorg. Chem.* **1980**, *19*, 518–524.
(45) Puget, K.; Michailson, A. M. *Biochimie* **1974**, *56*, 1255.
(46) Clarke, M. J. *Met. Ions Biol. Syst.* **1980**, *11*, 231–283.
(47) Clarke, M. J.; Pell, S. D.; Kumar, R., unpublished results.

Acknowledgment. We are grateful to Dr. Lloyd Taylor of the Polaroid Corp. for suggesting TMRA as a model for ascorbic acid and R. Salmonsen, who performed the preliminary NMR study. We also thank Dr. Hans Van Willigen of the University of Massachusetts, Boston, for collaborating on the EPR results. Funding for this work was provided by PHS Grant GM-26390.

Supplementary Material Available: Listings of initial rates and observed rate constants for the autoxidation of $[(NH_3)_5Ru(Asc)]^+$ and $[(NH_3)_5Ru(TMRA)]^+$, oxygen dependence of the autoxidation of $[(NH_3)_5Ru(Asc)]^+$ and $[(NH_3)_5Ru(TMRA)]^+$, observed rate constant and second-order specific rate constants for the autoxidation of reductate complexes as a function of temperature at pH 7, effect of superoxide dismutase and catalase on the autoxidation of ruthenium reductate complexes, the oxidation of $[(NH_3)_5Ru(TMRA)]^+$ and $[(NH_3)_5Ru(TMRA)]^+$ by hydrogen peroxide and oxygen, and reduction potential versus pH for $[(NH_3)_5Ru(TMRA)]^+$ and a figure of EPR of $[(Asc)(NH_3)_5Ru]^+$ (6 pages). Ordering information given on any current masthead page.

Crystal Chemistry of $Ba_2YCu_3O_7$ and Related Compounds

Michael O'Keeffe* and Staffan Hansen

Contribution from the Department of Chemistry, Arizona State University, Tempe, Arizona 85287. *Received June 4, 1987*

Abstract: The role of electropositive elements in stabilizing high oxidation states in crystals of transition elements such as copper is emphasized. An analysis of bond valences in the superconductor $Ba_2YCu_3O_7$ indicates that the valences of the two crystallographically distinct Cu atoms in the structure are intermediate between Cu(II) and Cu(III). Observed bond lengths, including the irregular coordination of Ba, can be understood when allowance is made for the differences in Cu–O bonds. A similar analysis of the insulating phase $Ba_2YCu_3O_6$ reveals well-defined Cu(I) and Cu(II) sites and rationalizes the presence of large displacements for two atoms in the structure. Defect structures in $Ba_2YCu_3O_7$ are discussed: bond lengths in a planar defect layer with composition $Ba_2Y_2Cu_4O_9$ are predicted and a model for {110} twinning is presented.

In view of the current intense interest in oxide superconductors it is worth examining their chemistry and structure from the point of view of a crystal chemist. This is done in this paper with particular emphasis on $Ba_2YCu_3O_7$, which is the highest temperature superconductor of which we are currently aware. First, attention is drawn to the role played by the larger, electropositive elements in stabilizing the structure and then attention is directed to the individual bond lengths and what they tell us about the atomic valences. We deliberately use the language of the solid-state chemist, with its strong bias to an intuitive "tight binding" description of the solid, rather than the band structure–oriented approach normally preferred by physicists.

Stabilization of High Valence States and/or Low Coordination Numbers

It has been documented elsewhere[1-3] that binary compounds, such as oxides, of particularly the heavier (more electropositive) alkali and alkaline earth metals (hereafter generically represented by A) are less stable to dissociation to atoms than might be expected from an examination of the thermodynamics of ternary etc. compounds involving also more-electronegative, higher valent elements (B). A plausible explanation has been offered[3] for this observation, but for our present purposes it is sufficient to note that compounds with a relatively high ratio of A atoms to anions X are less stable with respect to dissociation to atoms (or the normal elemental states) than those in which the corresponding ratio is less. Also relevant to the present discussion is the observation that a relatively large A/X ratio favors low coordination numbers for the cations B.[3]

We take a specific example to illustrate: K_2O has a much lower bond energy than expected from ternary etc. potassium oxides[1] and the coordination number of potassium by oxygen (four) in the binary oxide is significantly lower than is usually observed for potassium in oxides (eight to twelve). Now let us consider the following thermodynamic processes (it is irrelevant whether or not they can be realized directly in the laboratory).

For a process in which K_2O reacts with a high oxidation state transition metal oxide, e.g.

$$K_2O(s) + Cu_2O_3(s) \rightarrow 2KCuO_2(s) \qquad \Delta G^\circ < 0, \text{ say } -\gamma$$

Now consider

$$2CuO(s) + {}^1/_2O_2(g) \rightarrow Cu_2O_3(s) \qquad \Delta G^\circ_1 \qquad (1)$$

$$K_2O(s) + 2CuO(s) + {}^1/_2O_2(g) \rightarrow 2KCuO_2(s) \qquad \Delta G^\circ_2 = \Delta G^\circ_1 - \gamma \qquad (2)$$

In these equations s and g stand for solid and gaseous states. Elementary thermodynamic relationships then yield for the ratio of the oxygen equilibrium oxygen pressures for (1) and (2)

$$P_1/P_2 = \exp(2\gamma/RT) > 0 \qquad (3)$$

Thus it is expected to be easier (i.e., feasible at lower oxygen pressures) to obtain Cu(III) in the ternary compound with K than in a binary compound.[4] Indeed it is observed[5] that $KCuO_2$ can be prepared in 1 atm of oxygen at 450 °C, whereas it has not proved possible so far to prepare anhydrous Cu_2O_3 by direct combination of CuO and oxygen or indeed by any other means.[6] Many other examples of the stabilization of high oxidation states of transition metals when combined with alkaline or alkaline-earth oxides may be adduced.[3] Note that when an oxide like K_2O is heated in oxygen, because the K(II) level is so low lying, the oxygen is oxidized instead to peroxide.

The significance for the preparation of superconducting materials is that the combination of transition metals and large A

(1) O'Keeffe, M.; Stuart, J. A. *Inorg. Chem.* **1983**, *22*, 177.
(2) McGuire, N. K.; O'Keeffe, M. *J. Solid State Chem.* **1984**, *54*, 49.
(3) O'Keeffe, M.; Hyde, B. G. *Nature (London)* **1984**, *309*, 411.
(4) A reasonable estimate (1) for γ is ~200 kJ mol^{-1} so that at 1000 °C, $P_1/P_2 \sim 10^{16}$! Of course, eq 3 only holds in the limit of low pressures.
(5) Hestermann, K.; Hoppe, R. *Z. Anorg. Allg. Chem.* **1969**, *367*, 249.
(6) *Gmelins Handbook of Anorganische Chemie*; Verlag Chemie: Weinheim, 1958; Vol. 60, p 137.

0002-7863/88/1510-1506$01.50/0